N-WELL BASED CMOS CALORIMETRIC CHEMICAL SENSORS

N. Kerness, A. Koll, A. Schaufelbühl, C. Hagleitner, A. Hierlemann, O. Brand, and H. Baltes

Physical Electronics Laboratory, ETH Zurich, CH-8093 Zurich, Switzerland
Tel: +41-1- 633 2274, Fax: +41-1- 633 1054, email: kerness@iqe.phys.ethz.ch

ABSTRACT

New micromachined calorimetric chemical sensors based on an n-well island structure have been designed, fabricated in industrial CMOS technology, and tested. The suspended island structure is covered with a polymer and changes its temperature upon absorption or desorption of analyte. The temperature change is recorded by integrated polysilicon/aluminum thermopiles. A polysilicon or metal heating resistor covers the n-well structure which allows a more accurate calibration compared to our previous design [1]. The system provides a physical sensitivity of 34 and 26.5 mV/µW for the square and rectangular shaped membrane devices, respectively. Sensitivity and performance of the calorimetric chemical microsystem are shown by measurements for different volatile organic compounds. The system has a sensitivity of 0.045 and 0.049 mV/ppm to ethanol and 0.209 and 0.229 mV/ppm to toluene for the square and rectangular membrane devices, respectively.

INTRODUCTION

Calorimetric chemical sensors measure enthalpy changes which occur when an analyte is absorbed into or desorbed from a chemically sensitive layer, such as a polymer. Typically, the enthalpy changes cause a temperature change of a thermally insulated structure, which is sensed by a temperature sensor. Thereby, micromachined membrane structures in combination with thermopiles for temperature sensing is one possible approach [2, 3]. Fabricating calorimetric chemical sensors in a CMOS foundry provides the ability to produce reliable and potentially low cost sensors. Additionally, CMOS circuitry can be integrated on chip. In a post processing step the sensitive membrane is etched from the back side of the wafer. Since the device is fabricated in a commercial CMOS process, the formation of more diverse systems with multiple sensors relying on different sensing principles is possible [4]. The combination of these sensors can be referred to as an electronic nose [5].

In our previous design, the polymer layer was deposited onto a membrane comprising of the dielectric layer sandwich of the CMOS process. In this work (see Fig. 1 and Fig. 2), new calorimetric chemical sensors based on an n-well island structure have been designed, fabricated, and tested. The new design allows a more accurate calibration of the sensing system. This is supported by finite element simulations of the temperature distribution resulting from heat generated either in the heating resistor or in the poly-

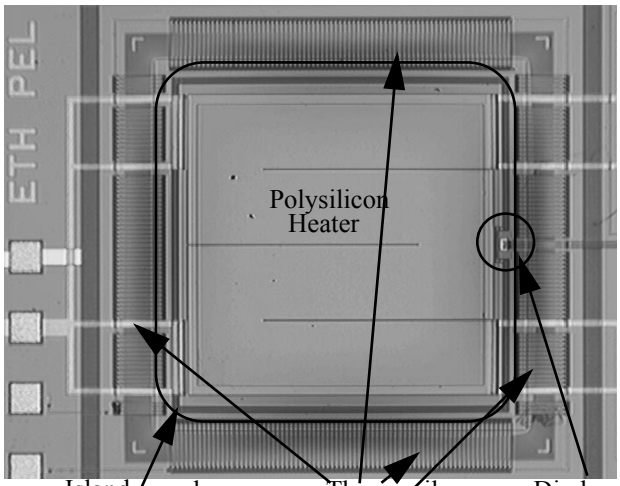

Figure 1: Micrograph of the chemical calorimetric sensor with a square n-well island structure, thermopile, polysilicon heater, and on-membrane diode. The island structures were released using a post-processing KOH etching step with electrochemical etch stop. The membrane is 1168 x 1168 µm^2 and features 274 thermocouples.

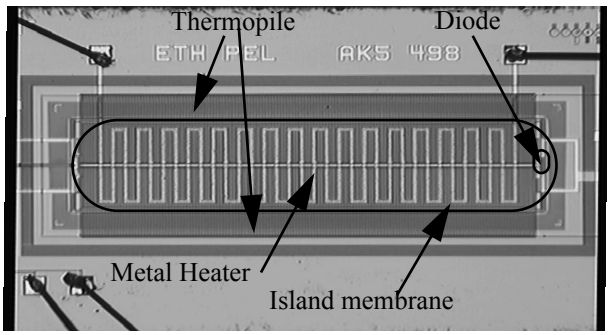

Figure 2: Micrograph of the chemical calorimetric sensor with a rectangular n-well island structure, thermopile, metal heater, and on-membrane diode. The membrane is 595 x 2162 µm^2 and features 300 thermocouples.

mer layer. Different volatile organic compounds are investigated with the new microsystem. The first results obtained with our improved measurement chamber exhibit an improvement in signal due to sharper switching of the analyte and carrier gas stream. The enthalpy [µJ] as a function of the analyte concentration [µmol/l] is given for toluene and ethanol.

SENSING PRINCIPLE

The steps for the detection of a concentration of analyte are as follows: (1) absorption of analyte based on the partion coefficient of the analyte/polymer combination, (2) generation of heat, (3) resulting temperature change of a thermally insulated structure, and (4) the thermovoltage change [2, 4]. The governing equation is analyte/polymer specific as well as device specific. The thermovoltage is proportional to the derivative of the concentration of the analyte as a function of time, dc_a/dt [mol/l·s], and is given by

$$\Delta V = m \cdot vol_{polymer} \cdot \overline{\Delta H}_{sum} \cdot K \cdot dc_a/dt \qquad (1)$$

where m [mV/µW] is the voltage versus heating power, the physical sensitivity of the device as it is mostly device dependent (steps 3 and 4), $vol_{polymer}$ is the volume of polymer (2), ΔH_{sum} is the generated molar absorption enthalpy according to the detected temperature change (2), and K is the partion coefficient (1). The generated enthalpy sum, ΔH_{sum}, is generally considered a combination of the molar enthalpy of mixing and the molar enthalpy of condensation [4, 6].

CMOS CALORIMETRIC DEVICES

The calorimetric devices are fabricated using a 0.8 µm CMOS process of Austria Mikro Systeme International, Austria in combination with post-process micromachining. Fig. 1 and Fig. 2 show the square and rectangular devices with the central n-well island structure and the thermopiles consisting of 274 and 300 thermocouples, respectively. The thermocouples are fabricated with the n-doped polysilicon and metal layers of the CMOS process, the Seebeck coefficient of the junction is approximately 111.3 ± 1.5 [µV/K] [7]. The thermocouple hot junction is located on the rim of the island structure and the cold junction is located on the bulk silicon, just beyond the edge of the membrane.

The n-well islands are suspended by a dielectric membrane and are released using a post-processing anisotropic KOH etching step with an electrochemical etch stop technique [8]. The etching is performed in a 6 molar KOH solution at 95 °C implementing a four-electrode configuration for the electrochemical etch-stop. The dielectric membrane is about 4 µm thick and the island structure is about 8 µm thick. The membranes are 1168 µm by 1168 µm and 595 µm by 2162 µm for the square and the rectangular sensors, respectively. In both cases the spacing from the edge of the membranes to the n-wells is 62.5 µm. Polysilicon (square membrane) and metal (rectangular membrane) heating resistors are located on the island structures for calibration. A schematic cross section of the rectangular membrane is shown in Fig. 3.

The new design has several advantages compared to our previous design [1]: the distributed heating resistor covers the same area as the polymer layer and, therefore, allows for a more accurate calibration of the chemical sensor; diodes are implemented on and off the membrane, allowing for precise temperature measurements; the use of the island structure in the membrane provides better mechanical stability and a more homogenous temperature distribution in the sensing area [8].

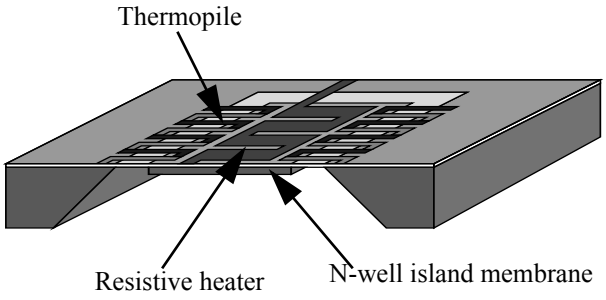

Figure 3: Schematic of the n-well based calorimetric sensor with suspended n-well island, polysilicon/metal thermopile and distributed heating resistor for calibration.

SIMULATION

The temperature distribution over the membranes has been simulated using the finite element software SOLIDIS [9]. The temperature profile (see Fig. 4) across the calorimetric sensor presented previously [1] and the n-well based devices have been simulated with heat generated either in the calibration resistor or the polymer. Due to symmetry only one quarter of the device is simulated. Fig. 5 compares the temperature profiles for the device with the square shaped island structure and the previously reported device [1] for a heating power of 1 µW generated in the polymer and the polysilicon heating resistors. For the n-well based device with distributed heating resistors, the temperature profile does not depend on whether the heat is dissipated in the polymer or the heating resistors. As a result, accurate calibration is possible. However, the maximum temperature elevation is higher for our previous devices, because of the lower thermal conductivity of the dielectric membrane.

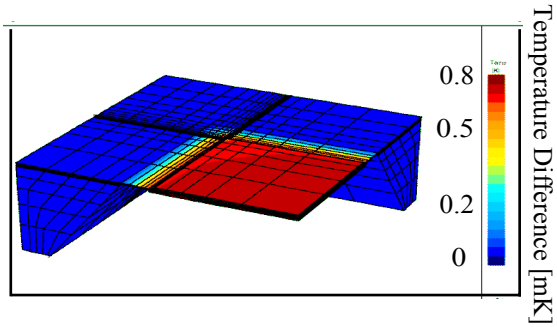

Figure 4: 3D simulation of the temperature profile in the device created by a heating power of 1µW in the polymer on top of the membrane. A quarter of the device has been simulated using the finite element program SOLIDIS.

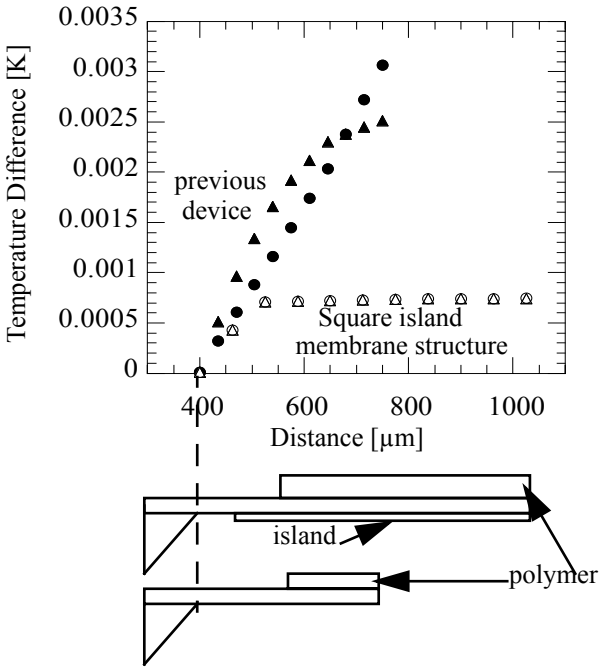

Figure 5: Simulated temperature profile across the square suspended island structure (hollow symbols) and the previous dielectric membrane (solid symbols) for a heating power of 1µW dissipated in the polymer (triangles) and the integrated polysilicon heating resistor (circles) for each sensor. Note that the 400 µm point is at the edge of the membrane on both devices and the previously reported device is more narrow than the square structured island membrane.

CHEMICAL CHARACTERIZATION

For chemical sensing, a polymer-covered sensing membrane and an uncovered reference membrane were connected in parallel to a low noise chopper stabilized instrumentation amplifier which features a gain of 2500 and a bandwidth of 500 Hz [10]. The sensor membrane was spray-coated through a shadow mask to control the placement and area of a 10 µm thick layer of poly(etherurethane) (PEUT, Thermedics, Woburn, MA, USA). After spray coating the sensors with PEUT from a 4mg/ml solution of dichloromethane, the sensors were cured for five minutes in an atmosphere saturated with dichloromethane in order to homogenize the layer. A sensor calibration with the integrated heating resistors yields physical sensitivities of 34 and 26.5 mV/µW for the square and rectangular island structured devices (Fig. 6). The physical sensitivity is the slope of the calibration, and is the term, m, in equation (1). Due to the slightly better thermal conductivity of the polymer coated sensing structures, the physical sensitivity of the sensor structures is about 1% smaller compared to the reference structures.

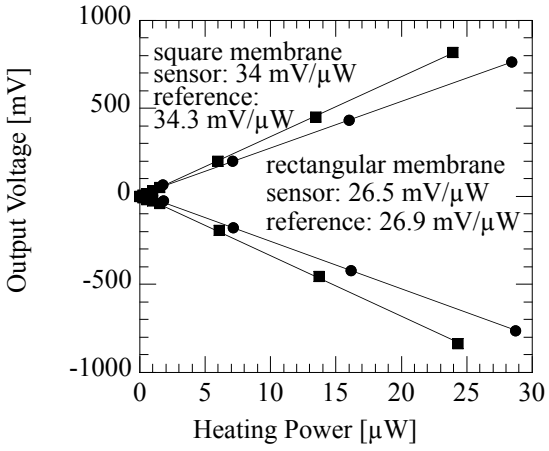

Figure 6: Physical sensitivity of the reference and the polymer coated sensor structures at 28 °C. The thermoelectric sensors were calibrated using polysilicon and metal heating resistors cointegrated on the square and rectangular island structured devices respectively.

The measurements were performed in a computer controlled flow manifold by pendulum switching between defined analyte concentrations and synthetic air as a reference gas at a constant flow rate of 33 ml/min [1]. The organic solvents were generated in thermostated vaporizers using synthetic air as a carrier gas. The gases were mixed and temperature stabilized before entering the measurement chamber. Two lines, one with pure carrier gas and one with air saturated with the analyte (to obtain a given concentration), were fed into a 4-way pendulum valve located close to the thermoregulated measurement chamber. The pendulum approach allows a fine-edged concentration of analyte to be delivered to the measurement chamber within a short time. This is especially advantageous for calorimetric sensors which are sensing transients in concentration.

RESULTS

Measurement cycles were performed for ethanol (Fig. 7), toluene (Fig. 8), and relative humidity (Fig. 9).

The positive and negative signal peaks are the enthalpy changes, which occur while switching the analyte on and off [11]. Thus the absorption and desorption of the analyte in the polymer is shown. In addition to the signals due to the analyte sorption and desorption there is another peak present in the measurements. The other peak is due to pressure or electrical effects caused by the valves. Steps are being taken to mitigate this spurious signal.

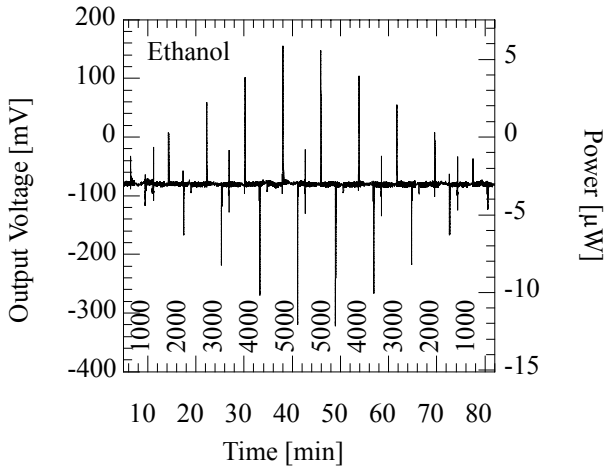

Figure 7: Measurement cycles for the rectangular shaped island structured devices with different concentrations of ethanol alternated with synthetic air at 33 ml/min and 28 °C. Concentrations are noted in [ppm]. The corresponding power was calculated using the calibration of Fig. 6.

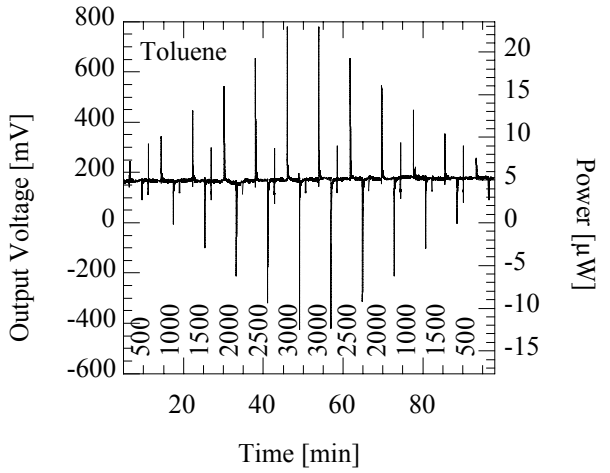

Figure 8: Measurement cycles for the square shaped island structured devices with different concentrations of toluene alternated with synthetic air at 33 ml/min and 28 °C. Concentrations are noted in [ppm].

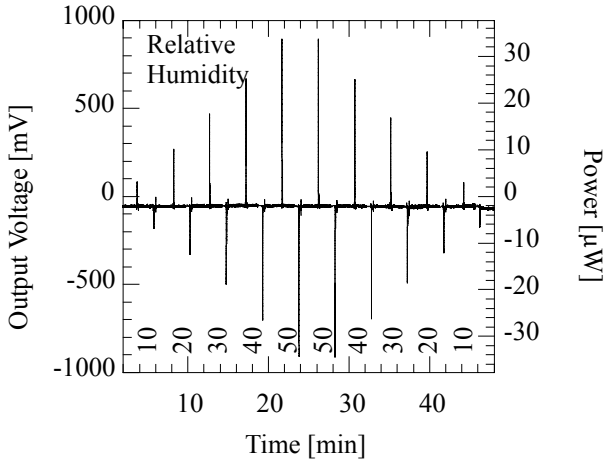

Figure 9: Measurement cycles for the rectangular shaped island structured devices exposed to different concentrations of relative humidity and synthetic air at 33 ml/min and 28 °C. Concentrations are noted in [% relative humidity].

The enthalpy changes are calculated by integration of the sensor output signal over time. A close up of the 1500 ppm toluene mixed with synthetic air on and off transient signals are shown in Fig. 10 and Fig. 11 for the rectangular devices. As expected, the resulting enthalpy changes are the same for switching on and off the analyte.

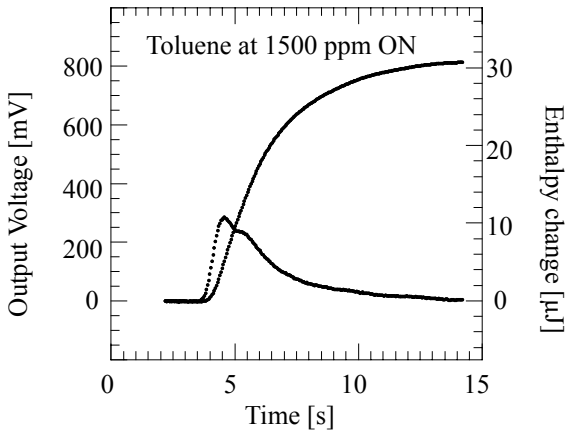

Figure 10: Measurement of the enthalpy change as synthetic air is switched (ON) to 1500 ppm toluene in synthetic air for the rectangular shaped island structured device. The enthalpy change was calculated by integrating the thermovoltage and utilizing the calibration data of Fig. 6.

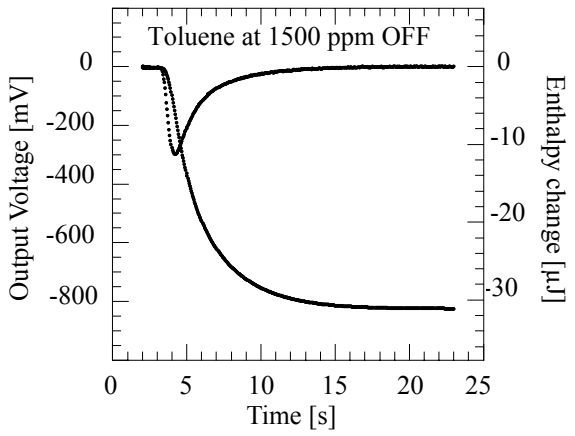

Figure 11: Measurement of the enthalpy change as 1500 ppm toluene in synthetic air is switched (OFF) to pure synthetic air for the rectangular shaped island structured device.

The maximum output voltage changes (peak maxima) are displayed in Fig. 12 as a function of the analyte concentration. Different slopes for ethanol and toluene reflect the different saturation vapor pressures and affinity of the polymer towards these analytes. Also the linearity is shown over the concentration regime measured. The slope of the peak voltage versus concentration for toluene is 0.209 mV/ppm and 0.229 mV/ppm for the square and rectangular shaped island structures, respectively. The slope of the peak voltage versus concentration for ethanol is 0.045 mV/ppm and 0.049 mV/ppm for the square and rectangular shaped island structures, respectively.

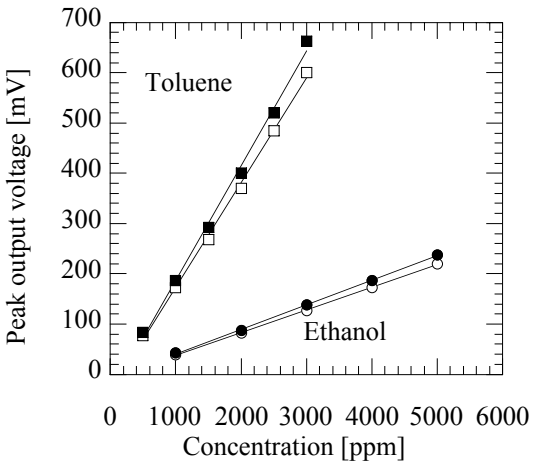

Figure 12: Peak output voltage for the rectangular (solid) and square (hollow) shaped island structured devices versus concentration in ppm.

Fig. 13 shows the enthalpy change [µJ] versus concentration [µmol/l]. The slope of the change in enthalpy versus concentration in the gas phase for toluene is 0.534 µJ/µmol/l and 0.570 µJ/µmol/l for the square and rectangular shaped island structures respectively. The slope of the change in enthalpy versus concentration for toluene is 0.103 µJ/µmol/l and 0.105 µJ/µmol/l for the square and rectangular shaped island structures, respectively. The molar enthalpy when the volume of polymer and the concentration in the polymer are considered amounts to 16.62 kJ/mol for ethanol and 33.79 kJ/mol for toluene, in the case of the rectangular shaped island devices, and 15.25 kJ/mol for ethanol and 29.73 kJ/mol for toluene, in the case of the square shaped island membranes. The results found here for toluene correspond well with the literature values for similar analyte/polymer combinations for the sum of condensation (exothermic, -37 kJ/mol) and mixing (endothermic +2 to +5 kJ/mol) molar enthalpies [5]. An exothermic enthalpy exhibits a heat given off by the polymer/analyte combination which is seen as a temperature increase in the calorimetric sensors.

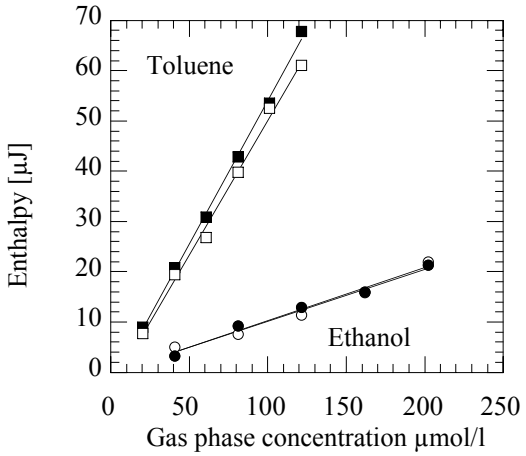

Figure 13: Change in enthalpy for the rectangular (solid) and square (hollow) shaped island structured devices versus analyte gas phase concentration in µmol/l.

CONCLUSIONS AND OUTLOOK

In summary, we have demonstrated an accurately calibrated CMOS calorimetric sensor. Since it is fabricated in a commercial CMOS process many advantages can be exploited: on chip circuitry, arrays of multiple sensing principle sensors can be combined on chip, low cost, low weight, and high reliability sensor systems can be realized. At present a detection limit of 118 ppm for toluene and 551 ppm for ethanol in the rectangular shaped island structured device is obtainable. This assumed a peak thermovoltage would be seen at three times the present noise voltage (9 mV peak to peak). This also corresponds to a heat detection lower limit of 2.72 µJ and 2.34 µJ for toluene and ethanol, respectively. Future work will include optimization of the sensor and sensor system, examination of other polymer/analyte combina-

tions for particular applications, and utilization of additional signal features.

ACKNOWLEDGMENTS

The authors greatly appreciate the help of current and former staff of the Physical Electronics Laboratory at ETH Zurich involved in chemical microsensor development directly and indirectly, specifically, Markus Emmenegger, Adrian Kummer, Dirk Lange, Matthias Metz, Thomas Müller, Donat Scheiwiller, Klaus Schneeberger, and Stefano Taschini. Additionally, the authors would like to acknowledge the excellent services of Austria Mikro Systeme International, Graz, Austria as the prototype manufacture. The financial support has been from the Koerber Foundation, Hamburg, Germany.

REFERENCES

[1] A. Koll, A. Schaufelbühl, N. Schneeberger, U. Münch, O. Brand, H. Baltes, C. Menolfi, Q.Huang, "Micromachined CMOS Calorimetric Chemical Sensor with On-Chip Low Noise Amplifier", MEMS '99, 547-551.

[2] A.W. van Herwaarden, P.M. Sarro, J.W. Gardner, P. Bataillard, "Liquid and Gas Micro-Calorimeters for (Bio)Chemical Measurements", Sensors and Actuators A, (1994) 24-30.

[3] D. Caspary, M. Schröpfer, J.Lerchner, G. Wolf, "A High Resolution IC-Calorimeter for Determination of Heats of Absorption onto Thin Coatings", Thermochimica Acta, in press.

[4] A. Hierlemann, A. Koll, D. Lange, C. Hagleitner, N. Kerness, O. Brand, and H. Baltes, "Application-Specific Sensor Systems Based on CMOS Chemical Microsensors", Sensors and Actuators B, submitted.

[5] J.W. Gardner, P.N. Bartlett, "A Brief History of Electronic Noses", Sensors and Actuators B 18-19, (1994) 211-220.

[6] A. Hierlemann, A.J. Ricco, K. Bodenhöfer, A. Dominik, and W. Göpel, "Conferring Selectivity to Chemical Sensors via Polymer Side Chain Selectivity", Analytical Chemistry, submitted.

[7] M. von Arx, "Thermal Properties of CMOS Thin Films", Ph.D. Thesis No.12743, ETH Zurich, 1998

[8] T. Müller, M. Brandl, O. Brand, and H. Baltes, "An Industrial CMOS Process Family Adapted for the Fabrication of Smart Silicon Sensors", Sensors and Actuators A, submitted.

[9] J.M. Funk, J.G. Korvink, J. Bühler, M. Bächtold, and H. Baltes, "SOLIDIS: A Tool for Microactuator Simulation in 3-D", J. MEMS, vol 6, 70-82, (1997).

[10] C. Menolfi and Q. Huang, "A Low-Noise CMOS Instrumentation Amplifier for Thermoelectric Infrared Detectors", IEEE J. Solid-State Circuits, vol SC-32, 968-976, 1997.

[11] M. Haug, K. D. Schierbaum, G. Gauglitz and W. Göpel, "Chemical Sensors Based upon Polysiloxanes: Comparison between Optical, Quartz microbalance, Calorimetric, and Capacitance Sensors", Sensors and Actuators B, 11, (1993) 383-391.